

Giant mesoscopic fluctuations of the elastic cotunneling thermopower of a single-electron transistor

A. S. Vasenko,¹ D. M. Basko,¹ and F. W. J. Hekking^{1,2}

¹University Grenoble Alpes, CNRS, LPMMC, F-38000 Grenoble, France

²Institut Universitaire de France, 103, bd Saint-Michel 75005 Paris, France

We study the thermoelectric transport of a small metallic island weakly coupled to two electrodes by tunnel junctions. In the Coulomb blockade regime, in the case when the ground state of the system corresponds to an even number of electrons on the island, the main mechanism of electron transport at the lowest temperatures is elastic cotunneling. In this regime, the transport coefficients strongly depend on the realization of the random impurity potential or the shape of the island. Using random-matrix theory, we calculate the thermopower and the thermoelectric kinetic coefficient and study the statistics of their mesoscopic fluctuations in the elastic cotunneling regime. The fluctuations of the thermopower turn out to be much larger than the average value.

PACS numbers: 73.23.Hk, 73.40.Gk, 73.50.Lw, 85.35.Gv

I. INTRODUCTION

Thermoelectric transport through various nanodevices has been the subject of extensive experimental and theoretical studies for more than two decades. The coherent propagation of electron waves in clean nanostructured conductors leads to quantum size effects that strongly affect the thermoelectric transport coefficients;¹ the presence of electron-electron interactions leads to additional renormalization phenomena.^{2,3} In low-dimensional disordered conductors, interference of diffusively scattered electron waves weakens the screening of electron-electron interactions, leading to anomalous, energy-dependent non-Fermi-liquid behavior of the thermoelectric transport coefficients.⁴ All these effects can be made visible explicitly using the tunability of nanodevices, *e.g.*, by varying external gate potentials or magnetic fields. Various practical applications based on thermoelectric phenomena in nanostructures have been developed, including thermometry, and nanorefrigeration,⁵⁻⁹ and more generally thermoelectric nanomachines.¹⁰⁻¹³

A prototypical device that manifests all the relevant aspects of electron transport in nanostructures, *i.e.*, quantum size effects, energy-dependent coherent propagation and electron-electron interaction effects, is the single-electron transistor (SET). It consists of an island (a quantum dot or a small metallic particle) connected to two leads (source and drain) by small tunnel junctions. The electrostatic potential on the island can be controlled externally due a capacitive coupling between the island and a nearby gate electrode with the capacitance C_g (Fig. 1). The electrostatic energy cost of putting an extra electron on the island is of the order of the so-called charging energy, $E_C \equiv e^2/2C$, where C is the total capacitance of the island. When the temperature T and the applied source-drain voltage V_{sd} are small, $eV_{sd}, T \ll E_C$, this charging effect results in the so-called Coulomb blockade of the electron transport through the island (see Ref. 14 for a review). Moreover, at low temperatures the electronic phase coherence length is longer than the typical

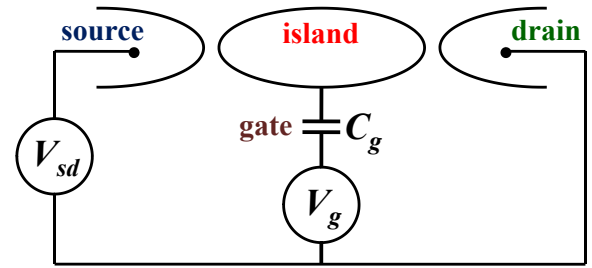


FIG. 1: (Color online) A sketch of a single-electron transistor. The central island is connected to the source and drain electrodes by tunnel junctions and capacitively coupled to the gate electrode via the gate capacitance C_g . The total capacitance C of the island is given by the sum of the capacitances between the island and each electrode.

dimensions of the island and as a result the electronic motion is phase-coherent.

The number of electrons N on the island that minimizes the electrostatic energy $E_{el}(N)$, as well as the energy cost $E_{el}(N \pm 1) - E_{el}(N)$ to add/remove an electron, depends on the external gate voltage V_g . For each N , there is a particular value of V_g , such that $E_{el}(N) = E_{el}(N+1)$, called the degeneracy point. Then, starting from the state with N electrons, one electron can tunnel from the source to the island, and then another electron tunnel from the island to the drain, restoring the number of electrons on the island to N . This so-called sequential tunneling mechanism (when electrons tunnel one by one in and out of the island, hence the term “single-electron transistor”) leads to a sequence of peaks in the dependence of the source-drain linear-response conductance G on V_g , spaced at e/C_g , schematically shown in Fig. 2a.

If V_g is tuned away from the degeneracy point into the Coulomb blockade valley, the sequential-tunneling contribution to the conductance is exponentially suppressed at low temperatures,^{15,16} and a more important contribution to the transport arises from the so-called cotunnel-

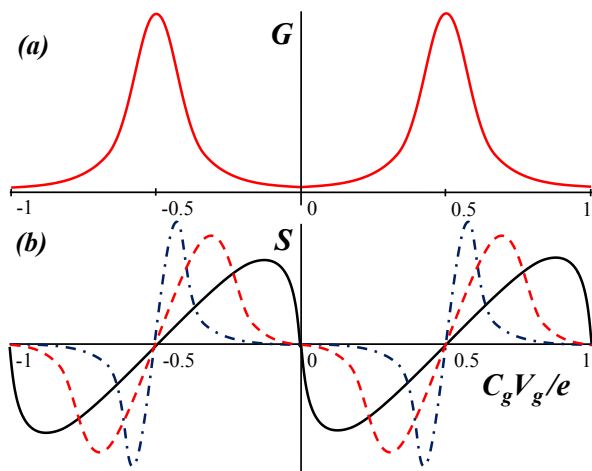


FIG. 2: (Color online) Schematic view of the dependence of the SET's conductance (a) and thermopower (b) on the dimensionless gate voltage $C_g V_g / e$. The three curves in panel (b) correspond to different temperatures, the black solid line corresponding to the highest temperature, the blue dash-dotted line to the lowest.

ing mechanism. It is due to processes where an electron tunnels from the source to the drain via a virtual intermediate state on the island. The energy of this virtual state is higher than that of the initial and final states by a large amount $\sim E_C$, so the tunneling amplitude is small as $\sim 1/E_C$. Yet, at low temperatures, this dominates over the exponentially small sequential-tunneling contribution $\sim \exp(-E_C/T)$.

If the internal state of the island (i. e., the distribution of the N electrons over the single-particle energy levels on the island) is different before and after the process, one speaks of inelastic cotunneling, in the opposite case it is called elastic cotunneling.^{17–20} As the inelastic cotunneling process involves creation of an electron-hole pair on the island, the corresponding contribution to the linear-response conductance vanishes at $T \rightarrow 0$ ($\propto T^2$), while the elastic one is temperature-independent. Thus, the latter dominates the transport at very low temperatures.²¹ An important difference between inelastic and elastic cotunneling is that the latter is sensitive to the coherent electron motion on the island whereas the former is not. As a result, the elastic cotunneling contribution to the SET's conductance shows strong mesoscopic sample-to-sample fluctuations,²² the fluctuations being of the same order as the average conductance. Moreover, the conductance fluctuations of elastic cotunneling are so large that they dominate the inelastic mechanism even at not too low temperatures, when the average conductance value is already determined by inelastic cotunneling.²² The noise of the cotunneling current through one or several tunnel-coupled quantum dots in the Coulomb blockade regime was calculated in Ref. 23.

The thermoelectric properties of SETs have been investigated in part, both theoretically and experimentally. The thermoelectric kinetic coefficient $G_T = I/\delta T$ is de-

efined as the response of the source-drain electric current I to a small temperature difference δT between the source and the drain at zero voltage, $V_{sd} = 0$. The thermopower $S = -V_{sd}/\delta T$ determines the voltage response to δT at zero electric current, $I = 0$ (that is, with disconnected external circuit in Fig. 1). In the sequential tunneling regime, the thermopower was predicted to exhibit periodic sawtooth oscillations as a function of V_g (see Ref. 24), as shown schematically in Fig. 2b (black solid line). This sawtooth behavior has been observed experimentally,^{25,26} however deviations from it have also been seen.^{27,28} The latter observations motivated the theoretical study of the inelastic cotunneling contribution to the thermopower.²⁹ It was shown that below some crossover temperature the thermopower in the valleys of Coulomb blockade is suppressed, the sawtooth behavior (black solid line in Fig. 2b) is strongly modified at low temperatures (blue dash-dotted line in Fig. 2b). Similar behavior was later observed experimentally.³⁰ Taking into account the inelastic cotunneling contribution also leads to the violation of the Wiedemann-Franz law in a SET device, as was theoretically shown in Ref. 31.

The elastic cotunneling contribution to thermopower was discussed in Refs. 32,33, but its statistics have not been properly analyzed. At the same time, given the fact that the elastic cotunneling regime gives rise to strong mesoscopic conductance fluctuations, it appears crucial to study the statistics of the thermoelectric coefficients in the elastic cotunneling regime. The purpose of the present work is to perform such a study. We consider thermoelectric transport through a small metallic island containing many electrons, whose discrete single-particle energy spectrum is characterized by the mean level spacing $\Delta \ll E_C$. This spectrum, as well as the coherent electron motion inside the dot, are assumed to be described by the orthogonal ensemble of the random matrix theory, corresponding to the absence of any external magnetic field. This assumption is valid as long as E_C is small compared to the Thouless energy of the island. At low temperatures, $T \ll \sqrt{E_C \Delta}$, we can neglect the contribution of the inelastic cotunneling.¹⁹ Under these assumptions, we determine (in the elastic cotunneling regime) the full statistics of the thermoelectric kinetic coefficient G_T^{el} and of the thermopower, $S^{el} = G_T^{el}/G^{el}$, and show that the fluctuations of S^{el} are much larger than the average value.

The paper is organized as follows. In Section II, we summarize the main results and discuss them qualitatively. We specify the model in Section III. The detailed calculations are presented in Section IV. We summarize results in Section V.

II. QUALITATIVE DISCUSSION AND SUMMARY OF THE MAIN RESULTS

Very generally, the linear response of charge and energy currents, I and J_E , to the voltage and temperature

differences, V and δT , is determined by the 2×2 matrix of the kinetic coefficients,

$$\begin{pmatrix} I \\ J_E \end{pmatrix} = \begin{pmatrix} G & G_T \\ K_V & K_T \end{pmatrix} \begin{pmatrix} V \\ \delta T \end{pmatrix}, \quad (1)$$

where $K_V = -TG_T$ due to the Onsager symmetry holding under time-reversal symmetry, thermopower $S = G_T/G$, and the thermal conductance K is given by $K = K_T - K_V G_T/G$. As will be shown in Sec. IV, for a given realization of the disorder or of the shape of the island and a given value of the gate voltage, the three independent kinetic coefficients in the regime of the elastic cotunneling can be represented in the form

$$G^{el} = \frac{G_s G_d}{4\pi e^2/\hbar} \frac{\Delta}{E_C} \tau^2(E_F), \quad (2a)$$

$$G_T^{el} = -\frac{\pi^2 T}{3e} \frac{G_s G_d}{4\pi e^2/\hbar} \frac{\Delta}{E_C} \frac{d\tau^2(E_F)}{dE_F}, \quad (2b)$$

$$K_T^{el} = \frac{\pi^2 T}{3e^2} \frac{G_s G_d}{4\pi e^2/\hbar} \frac{\Delta}{E_C} \tau^2(E_F). \quad (2c)$$

Here $G_s(G_d)$ is the conductance of the tunnel junction between the island and the source (drain) electrode. $\tau(E_F)$ is a smooth real dimensionless function of the Fermi energy E_F in the electrodes, which depends on the microscopic realization of disorder or the island shape, such as the one shown in Fig. 3. For a given realization, it varies on a typical energy scale E_C , and its typical value is ~ 1 (provided that the gate voltage is not too close to a degeneracy point). Thus, for a given realization, the kinetic coefficients satisfy the Mott formula for the thermopower and the Wiedemann-Franz law for K_T^{el} . This is quite natural, as these relations hold quite generally when the electron scattering is elastic.³⁴

As G^{el} and K_T^{el} depend on the realization via the same quantity $\tau^2(E_F)$, their statistics is identical. It was found in Ref. 22, where the distribution function of the elastic cotunneling electrical conductance G^{el} was found explicitly. Introducing the dimensionless variable $g = \tau^2(E_F)$, see Eq. (2a), it coincides with the Porter-Thomas distribution for the orthogonal ensemble,³⁵

$$P(g) = \Theta(g) \sqrt{\frac{1-4x^2}{4\pi g}} e^{-(1-4x^2)g/4}, \quad (3)$$

where $\Theta(g)$ is the Heaviside step function. Here, x is the rescaled gate voltage, such that $x = 0$ corresponds to the center of the Coulomb blockade valley, and $x = \pm 1/2$ corresponds to the two nearby degeneracy points. We restrict x to the interval $-1/2 < x < 1/2$, outside of which the dependence on the gate voltage should be periodically repeated. The average elastic cotunneling conductance value is given by Eq.(17) in Ref. 19,

$$\langle G^{el} \rangle = \frac{G_s G_d}{4\pi e^2/\hbar} \frac{\Delta}{E_C} \frac{2}{1-4x^2}, \quad (4)$$

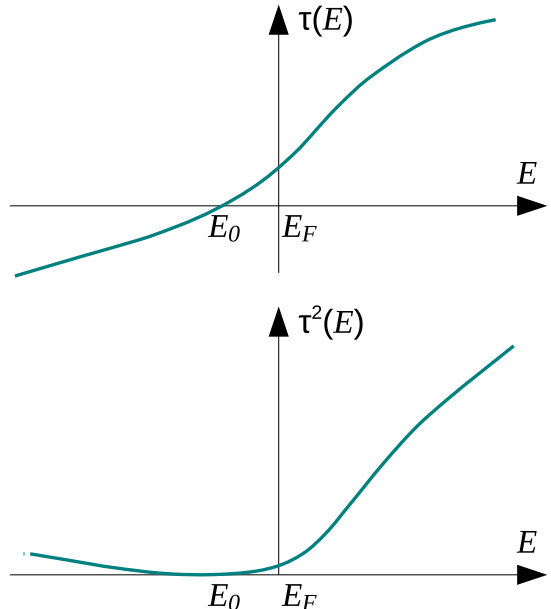


FIG. 3: (Color online) A sketch of possible behavior of the function $\tau(E)$ (upper panel) and the corresponding $\tau^2(E)$ (lower panel), entering Eq. (2a). The scale of the horizontal axis is $\sim E_C$, that of the vertical axis is ~ 1 .

and the fluctuations are indeed mesoscopically large, of the order of the average conductance,

$$\sqrt{\langle (G^{el})^2 \rangle - \langle G^{el} \rangle^2} = \sqrt{2} \langle G^{el} \rangle. \quad (5)$$

The quantity G_T^{el} depends on the realization via $d\tau^2(E_F)/dE_F$, therefore its statistics is different from that of G^{el} . However, these quantities are correlated. The consequence of this fact for the statistics of the thermopower can be understood from the following simple argument. The function $\tau(E)$ can have arbitrary sign, and it may even change sign at some point $E = E_0$ (Fig. 3). In the vicinity of E_0 , it can be approximated as $\tau(E) \approx A(E - E_0)$, where the coefficient A is non-singular. If E_0 happens to be close to E_F , then $G^{el} \propto \tau^2(E_F) \propto (E_F - E_0)^2$ is very small. As E_0 is random and determined by the island, while E_F is determined by the electrodes, E_0 can be assumed uniformly distributed in the vicinity of E_F . This immediately results in the $1/\sqrt{G^{el}}$ behavior of the distribution function of $G^{el} \propto A^2(E_F - E_0)^2$ at $G^{el} \rightarrow 0$, as found in Ref. 22 in the orthogonal ensemble. At the same time, the thermoelectric coefficient $G_T^{el} \propto d\tau^2(E_F)/dE_F \propto (E_F - E_0)$, so the thermopower $S^{el} = G_T^{el}/G^{el} \propto 1/(E_F - E_0)$. For a uniformly distributed E_0 , this gives $\alpha/(S^{el})^2$ for the asymptotics of the distribution function at $S^{el} \rightarrow \pm\infty$ with some coefficient α . As the coefficient is the same at $S^{el} \rightarrow +\infty$ and $S^{el} \rightarrow -\infty$, such a distribution has a finite first moment $\langle S^{el} \rangle$, but a divergent second moment $\langle (S^{el})^2 \rangle$, leading indeed to large mesoscopic fluctuations

of S^{el} . As we have just seen, these large fluctuations are dominated by those realizations where E_0 and E_F happen to be close to each other, that is, the electrical conductance is anomalously small.

These simple arguments are confirmed by the explicit calculation in Sec. IV, which gives the average elastic cotunneling thermopower,

$$\langle S^{el} \rangle = -\frac{\pi^2 T}{3eE_C} \frac{4x}{1-4x^2}, \quad (6)$$

and divergent higher moments. Note that $\langle S^{el} \rangle = 0$ at $x = 0$, since in the valley center the system is electron-hole-symmetric *on the average*. However, for any given realization, the electronic energy spectrum on the island does not have any symmetry, so there is no reason for S^{el} to vanish at $x = 0$ in any specific realization. Near the degeneracy points $x = \pm 1/2$, Eq. (6) gives a divergence, but in this region our theory does not work any more as the dominant contribution to the transport comes from the sequential tunneling mechanism. The full distribution function of the thermopower turns out to be a simple Lorentzian, conveniently written in terms of the dimensionless variable s , such that $S^{el} = -[\pi^2 T / (3eE_C)]s$:

$$P(s) = \frac{\sqrt{4/3}}{\pi} \frac{1-4x^2}{4/3 + [(1-4x^2)s - 4x]^2}. \quad (7)$$

We have also determined the full distribution function of G_T^{el} written here in terms of a dimensionless variable $g_T = E_C d\tau^2(E_F)/dE_F$ [see Eq. (2b)],

$$P(g_T) = \frac{\sqrt{3}}{4\pi} (1-4x^2)^2 \exp\left(\frac{3}{2}x(1-4x^2)^2 g_T\right) \times K_0\left(\frac{\sqrt{3}}{4}(1-4x^2)^2 \sqrt{1+12x^2} |g_T|\right), \quad (8)$$

where K_0 is the modified Bessel function. The corresponding average value is given by

$$\langle G_T^{el} \rangle = -\frac{\pi^2 T}{3e} \frac{G_s G_d}{4\pi e^2 / \hbar} \frac{\Delta}{E_C^2} \frac{4x}{(1-4x^2)^2}, \quad (9)$$

and higher moments are given by Eq. (43). Note that $\langle G_T^{el} / G^{el} \rangle = 2\langle G_T^{el} \rangle / \langle G^{el} \rangle$. In Fig. 4 we plot $P(g_T)$ for two different values of the dimensionless gate voltage $x = 0, 0.3$. Note that changing the sign $x \rightarrow -x$ amounts to $P(g_T) \rightarrow P(-g_T)$.

As G^{el} and G_T^{el} are correlated random variables, the full information about their statistics at a given value of x is provided by the joint distribution function, for which we have obtained the following analytical expression:

$$P(g, g_T) = \frac{\sqrt{3}\Theta(g)}{8\pi g} (1-4x^2)^2 \exp\left(-\frac{1-4x^2}{4}g\right) \times \exp\left\{-\frac{3(1-4x^2)[4x(1-4x^2)g - g_T]^2}{16g}\right\}. \quad (10)$$

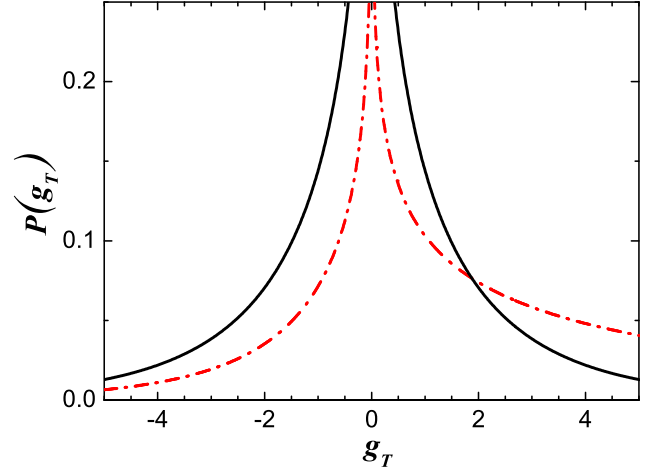


FIG. 4: (Color online) The distribution function $P(g_T)$ for $x = 0$ (black solid line) and $x = 0.3$ (red dash-dotted line).

To characterize statistical correlations at different values of x , one should consider $g(x)$ and $g_T(x)$ as two correlated random processes. They can be conveniently characterized in terms of

$$\tau_x = \sqrt{g(x)} = \tau(E_F), \quad \varepsilon_x = \frac{g_T(x)}{2\sqrt{g(x)}} = E_C \frac{d\tau(E_F)}{dE_F}, \quad (11)$$

which turn out to be Gaussian random processes with zero averages and pair correlators

$$\langle \tau_{x_1} \tau_{x_2} \rangle = \frac{1}{2(x_1 - x_2)} \ln \left(\frac{1+2x_1}{1-2x_1} \frac{1-2x_2}{1+2x_2} \right), \quad (12a)$$

$$\langle \tau_{x_1} \varepsilon_{x_2} \rangle = \frac{1}{(x_1 - x_2)(1-4x_2^2)} + \frac{1}{4(x_1 - x_2)^2} \ln \left(\frac{1+2x_1}{1-2x_1} \frac{1-2x_2}{1+2x_2} \right), \quad (12b)$$

$$\langle \varepsilon_{x_1} \varepsilon_{x_2} \rangle = \frac{1-2x_1^2-2x_2^2}{(x_1-x_2)^2(1-4x_1^2)(1-4x_2^2)} - \frac{1}{4(x_1-x_2)^3} \ln \left(\frac{1+2x_1}{1-2x_1} \frac{1-2x_2}{1+2x_2} \right). \quad (12c)$$

The divergence of mesoscopic fluctuations of the thermopower, found in the present work, originates from the fact that the elastic cotunneling contribution to the electrical conductance, calculated in the leading order in the tunneling couplings, has too high a probability to vanish. Indeed, as discussed in the paragraph preceding Eq. (6), both G^{el} and G_T^{el} may be small for some realizations, but it is easier for G^{el} to have an anomalously small value, than for G_T^{el} , and then their ratio $S^{el} = G_T^{el}/G^{el}$ becomes anomalously large. One should recall, however, that the leading-order elastic cotunneling is not the only contribution to the conductance. There are other contributions (e. g., the inelastic cotunneling,

or higher-order contributions to the elastic one), which work as parallel conduction channels, so the conductance never vanishes exactly. These contributions will cut off the divergence of $\langle S^2 \rangle$. Nevertheless, the fluctuations will still be parametrically large. To estimate the magnitude of the effect, let us assume that the elastic cotunneling conductance is shunted by the inelastic one,¹⁹ $G^{in} \sim (G_s G_d \hbar / e^2) (T^2 / E_C)^2$. The thermopower fluctuations will be determined by those realizations which have $G^{el} \sim G^{in}$, that is, $g \sim T^2 / (E_C \Delta) \ll 1$. Then the typical value of $g_T \sim \sqrt{g}$, as seen from Eq. (10). Thus, we can estimate $\sqrt{\langle S^2 \rangle} / \langle S \rangle \sim g_T / g \sim \sqrt{E_C \Delta} / T$. This factor is large precisely in the regime when the elastic cotunneling dominates over the inelastic one. Taking the values corresponding to the experiment of Ref. 30, $E_C = 1.5$ meV, $\Delta = 0.05$ meV, $T \sim \Delta \approx 0.6$ K, and $G_s = G_d = 0.012 e^2 / \hbar$, we have $\sqrt{E_C \Delta} / T \sim 5$. At lower temperatures, $T \ll \Delta$, the inelastic cotunneling is suppressed even stronger, so the fluctuations of the thermopower will be even larger.

At the same time, the effect of elastic cotunneling on the average thermopower is not very dramatic. Even at $T \ll \sqrt{E_C \Delta}$ when the inelastic contributions G^{in}, G_T^{in} are small compared to the typical values of the elastic ones, $G^{in} \ll G^{el}$, $|G_T^{in}| \ll |G_T^{el}|$, the ratios $S^{in} = G_T^{in} / G^{in}$ and $\langle S^{el} \rangle = \langle G_T^{el} / G^{el} \rangle$ are of the same order. Indeed, the average elastic cotunneling thermopower, given by Eq. (6), differs from the inelastic one, given by Eq. (23) in Ref. 29,

$$S^{in} = -\frac{4\pi^2 T}{5eE_C} \frac{4x}{1-4x^2}, \quad (13)$$

just by a constant factor 12/5. To illustrate this effect, we include sequential tunneling and inelastic cotunneling contributions to the conductance (G^{sq}, G^{in}) and to the thermoelectric kinetic coefficient (G_T^{sq}, G_T^{in}), and calculate the average of the total thermopower,

$$\langle S \rangle = \left\langle \frac{G_T^{sq} + G_T^{in} + G_T^{el}}{G^{sq} + G^{in} + G^{el}} \right\rangle, \quad (14)$$

which is straightforwardly evaluated from the joint distribution function (10). Taking G^{sq} and G_T^{sq} from Eqs. (13) and (14) in Ref. 29, respectively, and G^{in} and G_T^{in} from Eq. (10) in Ref. 19 and Eq. (22) in Ref. 29, we plot in Fig. 5 the average $\langle S \rangle$ for the values of the parameters from the experiment of Ref. 30, listed above, with and without elastic cotunneling contributions. Thus, the qualitative shape of the dependence of the average $\langle S \rangle$ on the gate voltage is the same as in the elastic cotunneling case, shown in Fig. 2b. However, for any specific realization of the quantum dot, the dependence of S will be different. In particular, there is no reason why it would vanish exactly in the center of the valley.

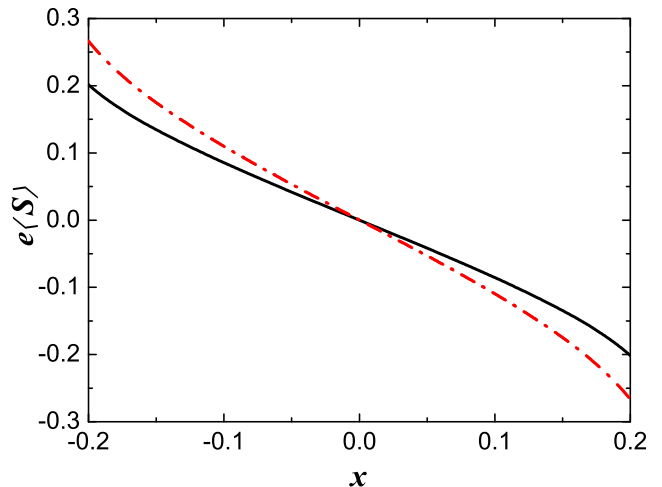


FIG. 5: (Color online) The averaged total thermopower with (black solid line) and without (red dashed line) taking into account the elastic cotunneling contributions. The difference of two curves is most visible in the interval $-0.2 < x < 0.2$. See the text for details.

III. THE MODEL

We model the single-electron transistor using the standard Hamiltonian¹⁴,

$$\hat{H} = \hat{H}_0 + \hat{H}_{Ts} + \hat{H}_{Td}, \quad (15a)$$

$$\hat{H}_0 = \sum_{\alpha=s,d} \sum_n \xi_{\alpha,n} \hat{c}_{\alpha,n}^\dagger \hat{c}_{\alpha,n} + \sum_k \epsilon_k \hat{b}_k^\dagger \hat{b}_k + \hat{H}_C, \quad (15b)$$

$$\hat{H}_{T\alpha} = \sum_{k,n} \left(t_{\alpha,kn} \hat{c}_{\alpha,n}^\dagger \hat{b}_k + t_{\alpha,kn}^* \hat{b}_k^\dagger \hat{c}_{\alpha,n} \right). \quad (15c)$$

Here the subscript $\alpha = s, d$ labels the two electrodes (source and drain, respectively), n and k label the single-electron states in the leads and on the island, respectively. For the sake of compactness, we suppress the spin indices. As we will not consider spin-flip processes, all subsequent calculations can be understood as performed for a given spin projection, and the final expressions for the transport coefficients will be multiplied by 2. $\hat{c}_{\alpha,n}$ and \hat{b}_k are the electron annihilation operators for the corresponding states, and the corresponding single-electron energies $\xi_{\alpha,n}, \epsilon_k$ are measured from the Fermi level.

\hat{H}_C in Eq. (15b) is the Coulomb interaction Hamiltonian for electrons on the island, obtained from the standard considerations.³⁶ Namely, the electrostatic energy E_{el} is assumed to be determined by the total electric charge $Q = -Ne$ on the island, $E_{el}(Q) = \int^Q \varphi(Q') dQ'$, where $\varphi(Q) = Q/C + C_g V_g / C$ is the electrostatic potential on the island, and $C = C_g + C_s + C_d + C_i$ is the total capacitance of the island, given by the sum of the capacitances to the gate (C_g), source (C_s), and drain (C_d) electrodes, as well as the self-capacitance C_i of the island.

Thus, \hat{H}_C can be written as

$$\hat{H}_C = E_C(\hat{N}^2 - 2\hat{N}C_g V_g/e), \quad \hat{N} = \sum_k \left[\hat{b}_k^\dagger \hat{b}_k - \Theta(-\epsilon_k) \right]. \quad (16)$$

Here $\Theta(-\epsilon)$ is the Heaviside step function, so \hat{N} is the operator of the *excess* number of electrons on the island, the charge of the filled Fermi sea at $\epsilon_k < 0$ assumed to be compensated by the neutralizing background. The degeneracy between states with N and $N + 1$ on the island occurs when the dimensionless gate voltage x is half-integer:

$$x \equiv \frac{C_g V_g}{e} = N + 1/2. \quad (17)$$

As the dependence of the transport coefficients on V_g is periodic, we can restrict our attention to the interval $-1/2 < x < 1/2$, where the Coulomb energy is minimized by $N = 0$. Thus, x measures the relative distance from the center of the Coulomb blockade valley. It is convenient to introduce the Coulomb energy cost of adding/removing one electron to/from the island,

$$E_\pm = E_{el}(N = \pm 1) - E_{el}(N = 0) = E_C(1 \mp 2x). \quad (18)$$

The matrix elements $t_{\alpha, kn}$ describe weak tunneling coupling between the electrodes and the island. Analogously to Ref. 22, we assume that this coupling is due to small overlap between the wave functions in the island and in each electrode α , dominated by the vicinity of a single point \mathbf{r}_α , where the island touches the electrode α . Then the tunneling Hamiltonian can be assumed to have the form

$$\hat{H}_{T\alpha} = t_\alpha \hat{\psi}_\alpha^\dagger(\mathbf{r}_\alpha) \hat{\Psi}(\mathbf{r}_\alpha) + t_\alpha^* \hat{\Psi}^\dagger(\mathbf{r}_\alpha) \hat{\psi}_\alpha(\mathbf{r}_\alpha), \quad (19)$$

where $\hat{\Psi}(\mathbf{r})$ and $\hat{\psi}_\alpha(\mathbf{r})$ are the fermionic field operators for the electrons on the island and in the contacts, respectively, and t_α are the tunneling amplitudes incorporating all necessary normalization factors. Expanding the fermionic operators in terms of the corresponding single-particle wave functions, $\Psi_k(\mathbf{r})$ and $\psi_{\alpha, n}(\mathbf{r})$, as

$$\hat{\Psi}(\mathbf{r}) = \sum_k \hat{b}_k \Psi_k(\mathbf{r}), \quad \hat{\psi}_\alpha(\mathbf{r}) = \sum_n \hat{c}_{\alpha, n} \psi_{\alpha, n}(\mathbf{r}), \quad (20)$$

we obtain the following simple expression for the matrix elements $t_{\alpha, kn}$:

$$t_{\alpha, kn} = t_\alpha \Psi_k(\mathbf{r}_\alpha) \psi_{\alpha, n}^*(\mathbf{r}_\alpha). \quad (21)$$

The energies $\xi_{\alpha, n}$ are assumed to have continuous spectra, so the leads are characterized by the local densities of states (per spin)

$$\nu_\alpha(\epsilon) = \sum_n |\psi_{\alpha, n}(\mathbf{r}_\alpha)|^2 \delta(\epsilon - \xi_{\alpha, n}), \quad (22)$$

assumed to be self-averaging and energy-independent. The energies ϵ_k of the single-particle states on the island are discrete with the mean level spacing Δ ($2/\Delta$

being the ensemble average of the single-electron density of states on the island for both spin projections). The island wave functions $\Psi_k(\mathbf{r}_\alpha)$ are assumed to be real random variables, not correlated with the energies ϵ_k , and corresponding to the elements of a random orthogonal matrix uniformly distributed in the orthogonal group. To the leading order in the matrix size, they can be treated as real independent Gaussian random variables,¹⁴ whose statistics is entirely determined by the pair correlator

$$\langle \Psi_k(\mathbf{r}_\alpha) \Psi_{k'}(\mathbf{r}_{\alpha'}) \rangle = \delta_{kk'} \delta_{\alpha\alpha'}, \quad (23)$$

all normalization factors being absorbed in the tunneling amplitudes t_α in Eq. (21). Instead of t_α , it is convenient to characterize each tunneling contact by a physical quantity, such as its average conductance (including the factor of 2 from spin),

$$G_\alpha = 2 \frac{2\pi e^2}{\hbar} \frac{|t_\alpha|^2 \nu_\alpha}{\Delta}. \quad (24)$$

IV. CALCULATION

A. Transport coefficients for a given realization

Following Refs. 18,36, we start from the Golden Rule expression for the source-drain current, which represents the difference between the rate of electron transfer from state n on the source to the state m on the drain and the rate of the opposite process,

$$I = -2e \sum_{n, m} [f_s(\xi_{s, n}) - f_d(\xi_{d, m})] \times |M_{s, n \rightarrow d, m}|^2 \frac{2\pi}{\hbar} \delta(\xi_{s, n} - \xi_{d, m}), \quad (25)$$

where we used the fact that the cotunneling matrix element $M_{d, m \rightarrow s, n} = M_{s, n \rightarrow d, m}^*$ and took into account the spin degeneracy. In Eq. (25), $f_\alpha(\xi)$ is the average occupation probability of the state with energy ξ on the electrode α :

$$f_\alpha(\xi) = \frac{1}{1 + e^{(\xi - \mu_\alpha)/T_\alpha}}. \quad (26)$$

Focusing on the linear response to small chemical potential and temperature differences, $\mu_s - \mu_d = -eV$, $T_s - T_d = \delta T$, we can write

$$I = \frac{1}{\pi\hbar} \int (-e) \mathcal{T}(\xi) \left(-eV + \frac{\xi}{T} \delta T \right) \left(-\frac{\partial f_{eq}}{\partial \xi} \right) d\xi, \quad (27)$$

$$\mathcal{T}(\xi) = 4\pi^2 \sum_{nm} |M_{s, n \rightarrow d, m}|^2 \delta(\xi_{s, n} - \xi) \delta(\xi_{d, m} - \xi), \quad (28)$$

where $f_{eq}(\xi) = 1/[1 + \exp(\xi/T)]$. Using the same approach, one can also find the energy current J_E between

the source and the drain. The corresponding expression can be obtained from Eq. (27) by simply replacing the factor $(-e)$, which is nothing but the charge transferred in a single tunneling event, by the corresponding transferred energy ξ .

As will be seen below [Eq. (34)], $\mathcal{T}(\xi)$ is a smooth function of ξ varying on a typical scale of $\xi \sim E_C$. At the same time, $-\partial f_{eq}/\partial \xi$ is strongly peaked around zero on the scale $\xi \sim T$. Thus, at low temperatures, the elastic cotunneling kinetic coefficients, appearing in Eq. (1), can be approximated as

$$G^{el} = \frac{e^2}{\pi \hbar} \mathcal{T}(0), \quad (29a)$$

$$G_T^{el} = -\frac{e}{\pi \hbar} \frac{\pi^2 T}{3} \mathcal{T}'(0), \quad (29b)$$

$$K_T^{el} = \frac{1}{\pi \hbar} \frac{\pi^2 T}{3} \mathcal{T}(0), \quad (29c)$$

where we have used

$$\int \left(-\frac{\partial f_{eq}}{\partial \xi} \right) d\xi = 1, \quad \int \xi^2 \left(-\frac{\partial f_{eq}}{\partial \xi} \right) d\xi = \frac{\pi^2 T^2}{3}. \quad (30)$$

Note that in order to calculate G_T^{el} , one has to expand the transmission function $\mathcal{T}(\xi) \approx \mathcal{T}(0) + \xi \mathcal{T}'(0)$, as the leading term vanishes due to parity $\xi \rightarrow -\xi$.

The cotunneling matrix element $M_{s,n \rightarrow d,m}$ is evaluated in the second-order perturbation theory in the tunneling Hamiltonian $\hat{H}_T = \hat{H}_{T_s} + \hat{H}_{T_d}$ as^{18,36}

$$M_{s,n \rightarrow d,m} = \sum_v \frac{\langle \Phi | \hat{c}_{d,m} \hat{H}_T | v \rangle \langle v | \hat{H}_T \hat{c}_{s,n}^\dagger | \Phi \rangle}{E_\Phi + \xi_{s,n} - E_v}, \quad (31)$$

where $\hat{c}_{s,n}^\dagger | \Phi \rangle$ is the initial state of the system. It is conveniently represented as an extra electron on top of some reference many-body state $|\Phi\rangle$, defined by the occupation numbers of all single-particle states. The final state is represented as $\hat{c}_{d,m}^\dagger | \Phi \rangle$, an extra electron on top of the *same* reference state $|\Phi\rangle$, which is the characteristic of the *elastic* cotunneling process. The states $|v\rangle$ are virtual intermediate states with energies E_v . As \hat{H}_T changes the number of electrons on the island by one, the states $|v\rangle$ can belong to two sectors: those with one more electron on the island (which is thus added to some empty single-particle level k), and those with one less electron (which is thus removed from some filled single-particle level k).

Splitting the tunnel Hamiltonian Eq. (15c) as

$$\hat{H}_{T\alpha} = \hat{H}_{T\alpha-} + \hat{H}_{T\alpha+}, \quad (32a)$$

$$\hat{H}_{T\alpha-} = \sum_{k,n} t_{\alpha,kn} \hat{c}_{\alpha,n}^\dagger \hat{b}_k = \hat{H}_{T\alpha+}^\dagger, \quad (32b)$$

we note that the first sector can be coupled to the initial state only by the $\hat{H}_{T_{s+}}$ term, while the second sector only by the $\hat{H}_{T_{d-}}$ term. The energies of the intermediate states in the two sectors are given by

$$E_\Phi + E_+ + \epsilon_k, \quad E_\Phi + E_- - \epsilon_k + \xi_{s,n} + \xi_{d,m},$$

respectively, where the Coulomb energies E_\pm are defined in Eq. (18). Evaluation of the matrix elements gives

$$M_{s,n \rightarrow d,m} = \sum_k t_{d,km} t_{s,kn}^* \times \left(\frac{f_k}{E_- - \epsilon_k + \xi_{d,m}} - \frac{1 - f_k}{E_+ + \epsilon_k - \xi_{s,n}} \right), \quad (33)$$

where f_k is the occupation number of the single-electron state k in the many-body state $|\Phi\rangle$. It should be noted that, strictly speaking, in a given reference state $|\Phi\rangle$, f_k is either 0 or 1. Then, to obtain the statistics of the transport coefficients, averaging over different reference states $|\Phi\rangle$ should also be performed, which results in the probability of $f_k = 1$ to be given by $f_{eq}(\epsilon_k)$. However, this probability is different from 0 or 1 only in the range of energies $|\epsilon_k| \sim T$, while, as will be seen later, the sum over k in Eq. (33) is contributed by a much wider range, $|\epsilon_k| \sim E_C$. Thus, we approximate $f_k = \Theta(-\epsilon_k)$. The error introduced by this approximation is small by a factor $T/E_C \ll 1$.

Substituting Eq. (33) into Eq. (28) and using Eqs. (21), (22), and (24), we obtain

$$\mathcal{T}(\xi) = \frac{\hbar^2 G_s G_d}{4e^4} \left| \sum_k \rho_k \left[\frac{\Delta \Theta(\epsilon)}{E_+ + \epsilon - \xi} - \frac{\Delta \Theta(-\epsilon)}{E_- - \epsilon + \xi} \right] \right|^2, \quad (34)$$

where we denoted

$$\rho_k = \Psi_k(\mathbf{r}_s) \Psi_k^*(\mathbf{r}_d). \quad (35)$$

Using Eqs. (29a) and (29b), the transport coefficients G^{el} and G_T^{el} can be expressed as

$$G^{el} = \frac{G_s G_d}{4\pi e^2 / \hbar} X, \quad G_T^{el} = -\frac{\pi^2 T}{3e} \frac{G_s G_d}{4\pi e^2 / \hbar} Y, \quad (36a)$$

$$X = \sum_{k,k'} \rho_k \rho_{k'}^* F(\epsilon_k) F(\epsilon_{k'}), \quad (36b)$$

$$Y = \sum_{k,k'} \rho_k \rho_{k'}^* \left[F(\epsilon_k) \tilde{F}(\epsilon_{k'}) + \tilde{F}(\epsilon_k) F(\epsilon_{k'}) \right], \quad (36c)$$

$$F(\epsilon) = \frac{\Delta \Theta(\epsilon)}{E_+ + \epsilon} - \frac{\Delta \Theta(-\epsilon)}{E_- - \epsilon}, \quad (36d)$$

$$\tilde{F}(\epsilon) = \frac{\Delta \Theta(\epsilon)}{(E_+ + \epsilon)^2} + \frac{\Delta \Theta(-\epsilon)}{(E_- - \epsilon)^2}. \quad (36e)$$

The random variables τ_x, ε_x , defined in Eq.(11), are represented as

$$\tau_x = \sqrt{\frac{E_C}{\Delta}} \sum_k \rho_k F(\epsilon_k), \quad \varepsilon_x = \sqrt{\frac{E_C^3}{\Delta}} \sum_k \rho_k \tilde{F}(\epsilon_k). \quad (37)$$

B. Averaging over realizations

The statistics of the transport coefficients will be obtained from the joint moments of G^{el} and G_T^{el} , as it was

done in Ref. 22 for G^{el} alone. Thus, we need to average products of X 's and Y 's [defined in Eqs. (36b), (36c)] over the energies ϵ_k and wave function amplitudes $\Psi_k(\mathbf{r}_\alpha)$. This task is facilitated by the following two considerations.

(i) Strictly speaking, the positions of the random energy levels ϵ_k are correlated.³⁷ However, these correlations occur on the energy scale Δ . Thus, for any smooth function of energy, $\mathcal{F}(\epsilon)$, varying on the scale $\epsilon \sim E_C$, the sum over ϵ_k will be replaced by the integration over ϵ ,

$$\sum_k \mathcal{F}(\epsilon_k) \rightarrow \int \mathcal{F}(\epsilon) \frac{d\epsilon}{\Delta}. \quad (38)$$

This approximation introduces an error which is small by a factor Δ/E_C . Of particular importance for the future calculations will be the following three integrals:

$$\mathcal{J}_1 = \int F^2(\epsilon) \frac{d\epsilon}{\Delta} = \frac{\Delta}{E_+} + \frac{\Delta}{E_-}, \quad (39a)$$

$$\mathcal{J}_2 = \int F(\epsilon) \tilde{F}(\epsilon) \frac{d\epsilon}{\Delta} = \frac{\Delta}{2E_+^2} - \frac{\Delta}{2E_-^2}, \quad (39b)$$

$$\mathcal{J}_3 = \int \tilde{F}^2(\epsilon) \frac{d\epsilon}{\Delta} = \frac{\Delta}{3E_+^3} + \frac{\Delta}{3E_-^3}. \quad (39c)$$

(ii) When averaging over the wave function amplitudes $\Psi_k(\mathbf{r}_\alpha)$ (which is independent of the averaging over ϵ_k) using Eq. (23) in the orthogonal ensemble, strictly speaking, all possible pairings should be taken, in accordance with Wick's theorem for Gaussian random variables. However, the amplitudes enter X and Y via a combination $\rho_k = \Psi_k(\mathbf{r}_s) \Psi_k^*(\mathbf{r}_d)$. Then, for a product $\rho_{k_1} \dots \rho_{k_{2n}}$ [a product of an odd number of factors always vanishes because $\Psi_k(\mathbf{r}_s)$ and $\Psi_{k'}(\mathbf{r}_d)$ are uncorrelated], those pairings are more important, where $\Psi_{k_1}(\mathbf{r}_s) \dots \Psi_{k_{2n}}(\mathbf{r}_s)$ are paired exactly in the same way as $\Psi_{k_1}(\mathbf{r}_d) \dots \Psi_{k_{2n}}(\mathbf{r}_d)$, as it gives the minimal number of constraints on the indices. This happens because each summation is transformed into integration over a range of $\epsilon \sim E_C$, and thus produces a large factor $\sim E_C/\Delta$, as discussed in the previous paragraph.

To illustrate this fact, consider the average

$$\begin{aligned} \langle Y^2 \rangle &= 4 \sum_{k_1 \dots k_4} \langle \rho_{k_1} \rho_{k_2} \rho_{k_3} \rho_{k_4} \rangle F(\epsilon_{k_1}) F(\epsilon_{k_2}) \tilde{F}(\epsilon_{k_3}) \tilde{F}(\epsilon_{k_4}) \\ &= 4 \sum_{k_1 \dots k_4} F(\epsilon_{k_1}) F(\epsilon_{k_2}) \tilde{F}(\epsilon_{k_3}) \tilde{F}(\epsilon_{k_4}) \times \\ &\quad \times [\delta_{k_1 k_2} \delta_{k_3 k_4} + \delta_{k_1 k_3} \delta_{k_2 k_4} + 2\delta_{k_1 k_2} \delta_{k_1 k_3} \delta_{k_1 k_4}] \\ &= 4 \sum_{k, k'} F^2(\epsilon_k) \tilde{F}^2(\epsilon_{k'}) + \\ &\quad + 4 \sum_{k, k'} F(\epsilon_k) \tilde{F}(\epsilon_k) F(\epsilon_{k'}) \tilde{F}(\epsilon_{k'}) + \\ &\quad + 8 \sum_k F^2(\epsilon_k) \tilde{F}^2(\epsilon_k) \\ &= 4(\mathcal{J}_1 \mathcal{J}_3 + \mathcal{J}_2^2)[1 + O(\Delta/E_C)]. \end{aligned} \quad (40)$$

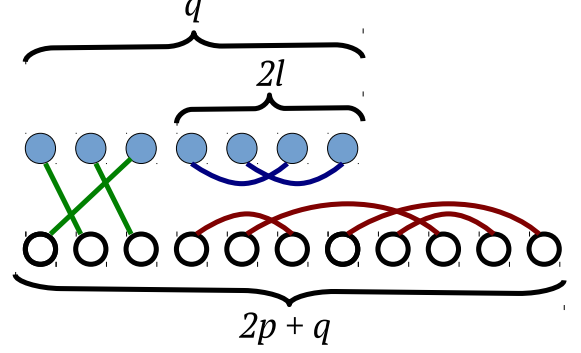


FIG. 6: (Color online) An example of pairing $2p+q$ F 's (shown by empty circles) and q \tilde{F} 's (filled circles).

The third term contains a single sum instead of a double sum, so its contribution is smaller by a factor Δ/E_C . Neglecting those pairings, which produce extra constraints on the indices, is equivalent to treating ρ_k 's as real independent Gaussian random variables with the pair correlator

$$\langle \rho_k \rho_{k'} \rangle = \delta_{kk'}. \quad (41)$$

Armed with this knowledge, we are now ready to calculate an arbitrary joint moment,

$$\begin{aligned} \langle X^p Y^q \rangle &= 2^q \sum_{k_1 \dots k_{2p+2q}} \langle \rho_{k_1} \dots \rho_{k_{2p+2q}} \rangle \\ &\quad \times F_1 \dots F_{2p+q} \tilde{F}_{2p+q+1} \dots \tilde{F}_{2p+2q}, \end{aligned} \quad (42)$$

where we denoted $F(\epsilon_{k_i}) = F_i$, $\tilde{F}(\epsilon_{k_i}) = \tilde{F}_i$ for compactness. Evaluation of the average $\langle \rho_{k_1} \dots \rho_{k_{2p+2q}} \rangle$ amounts to summation over all possible pairings of ρ_k 's. Each pairing of ρ_k 's induces a pairing of F_k 's and \tilde{F}_k 's, then the subsequent summation over the corresponding k index is performed independently from other indices, thereby producing a factor \mathcal{J}_1 for FF , \mathcal{J}_2 for $F\tilde{F}$, and \mathcal{J}_3 for $\tilde{F}\tilde{F}$, according to Eqs. (38) and (39a)–(39c).

Let us classify all possible pairings by the number $2l$ of all \tilde{F} 's which are paired among themselves, so that the remaining $q-2l$ \tilde{F} 's are paired with F 's, and the remaining $2p+2l$ F 's are also paired among themselves, as illustrated graphically in Fig. 6. Obviously, $0 \leq l \leq q/2$, and all pairings with a given l give a factor $\mathcal{J}_1^{p+l} \mathcal{J}_2^{q-2l} \mathcal{J}_3^l$. To determine the combinatorial coefficient, we first note that there are $q!/[(2l)!(q-2l)!]$ ways to choose $2l$ \tilde{F} 's out of q , and $(2p+q)!/[(q-2l)!(2p+2l)!]$ ways to choose $2p+2l$ F 's out of $2p+q$. Then, there are $(q-2l)!$ ways to pair up $q-2l$ F 's with $q-2l$ \tilde{F} 's, $(2l-1)!! = (2l)!/(2^l l!)$ ways to pair up the $2l$ \tilde{F} 's among themselves, and $(2p+2l-1)!! = (2p+2l)!/[2^{p+l}(p+l)!]$

ways to pair up the $2p + 2l$ F 's. As a result,

$$\langle X^p Y^q \rangle = \sum_{0 \leq l \leq q/2} \frac{2^{q-2l-p} q! (2p+q)!}{l! (q-2l)! (p+l)!} \mathcal{J}_1^{p+l} \mathcal{J}_2^{q-2l} \mathcal{J}_3^l. \quad (43)$$

From the joint moments, the full statistics can be reconstructed following the standard procedure (given in detail in the Appendix).

V. CONCLUSIONS

We have developed a quantitative theory of thermoelectric transport in a single electron transistor, consisting of a quantum dot weakly coupled to two electronic leads and capacitively coupled to a gate electrode, in the regime of elastic cotunneling. In this regime, the transport coefficients strongly depend on the realization of the random impurity potential or the shape of the island. We assumed the quantum dot wave functions to be Gaussian random variables and used the random-matrix theory for the orthogonal ensemble (i.e. in the absence of the magnetic field).

The distribution function of the conductance G was previously obtained by Aleiner and Glazman in Ref. 22. We have extended this result and calculated the distributions of the thermopower S , the thermoelectric kinetic coefficient G_T , and the joint distribution function of the conductance and thermoelectric kinetic coefficient as functions of the gate voltage. Statistical correlations of G and G_T at different values of the gate potential were also calculated.

Finally, we have calculated the average elastic cotunneling values of the thermopower and thermoelectric kinetic coefficient and the average values of all moments of G_T . We have shown that the second and higher moments of the thermopower diverge, which leads to large mesoscopic fluctuations of the elastic cotunneling thermopower. This divergence is cut off by taking into account the inelastic cotunneling contribution, or higher-order contributions to the elastic one. Nevertheless, the fluctuations will still be parametrically large.

We have estimated the magnitude of these fluctuations, taking into account the experimental parameters from Ref. 30, $\sqrt{\langle S^2 \rangle} / \langle S \rangle \sim 5$. Therefore for any specific realisation of the quantum dot, the dependence of S on the gate voltage will be different from $\langle S \rangle$. In particular, there is no reason why it would vanish exactly in the center of the Coulomb blockade valley.

VI. ACKNOWLEDGEMENTS

The authors are grateful to D.V. Averin, V. Bujanja, R. Whitney, and C. Winkelmann for helpful discussions. This work was supported by European Union Seventh Framework Programme (FP7/2007–2013) under grant

agreement ‘‘INFERNOS’’ No. 308850, as well as by Institut Universitaire de France.

Appendix A: Statistics from joint moments

From the joint moments (43), we first reconstruct the characteristic function:

$$\begin{aligned} \chi(u, v) &= \langle e^{-iuX - ivY} \rangle = \sum_{p, q=0}^{\infty} \frac{(-iu)^p (-iv)^q}{p! q!} \langle X^p Y^q \rangle \\ &= \sum_{p=0}^{\infty} \sum_{l=0}^{\infty} \sum_{q=2l}^{\infty} \frac{(2p+q)!}{p! (p+l)! l! (q-2l)!} \\ &\quad \times (-iu \mathcal{J}_1/2)^p (-v^2 \mathcal{J}_1 \mathcal{J}_3)^l (-2iv \mathcal{J}_2)^{q-2l} \\ &= \frac{1}{1 + 2iv \mathcal{J}_2} \sum_{p=0}^{\infty} \sum_{l=0}^{\infty} \frac{(2p+2l)!}{p! (p+l)! l!} \\ &\quad \times \left[\frac{-iu \mathcal{J}_1/2}{(1 + 2iv \mathcal{J}_2)^2} \right]^p \left[\frac{-v^2 \mathcal{J}_1 \mathcal{J}_3}{(1 + 2iv \mathcal{J}_2)^2} \right]^l \\ &= \frac{1}{1 + 2iv \mathcal{J}_2} \sum_{s=0}^{\infty} \frac{(2s)!}{(s!)^2} \left[\frac{-iu \mathcal{J}_1/2 - v^2 \mathcal{J}_1 \mathcal{J}_3}{(1 + 2iv \mathcal{J}_2)^2} \right]^s \\ &= \frac{1}{\sqrt{(1 + 2iv \mathcal{J}_2)^2 + 2iu \mathcal{J}_1 + 4v^2 \mathcal{J}_1 \mathcal{J}_3}}. \quad (A1) \end{aligned}$$

The sums were calculated using the following relations:

$$\sum_{n=0}^{\infty} \frac{(m+n)!}{n!} z^n = \frac{m!}{(1-z)^{m+1}}, \quad (A2a)$$

$$\begin{aligned} \sum_{m, n=0}^{\infty} \frac{\mathcal{F}(m+n)}{m! n!} x^m y^n &= \sum_{N=0}^{\infty} \sum_{k=0}^N \frac{\mathcal{F}(N)}{k! (N-k)!} x^k y^{N-k} \\ &= \sum_{N=0}^{\infty} \frac{\mathcal{F}(N)}{N!} (x+y)^N, \quad (A2b) \end{aligned}$$

$$\sum_{n=0}^{\infty} \frac{(2n)!}{(n!)^2} z^n = \frac{1}{\sqrt{1-4z}}. \quad (A2c)$$

From the characteristic function, the probability distributions can be determined. For the conductance,

$$P(X) = \int \frac{du}{2\pi} e^{iuX} \chi(u, 0) = \frac{\Theta(X) e^{-X/(2\mathcal{J}_1)}}{\sqrt{2\pi \mathcal{J}_1 X}} \quad (A3)$$

coincides with the result of Ref. 22 for the orthogonal ensemble. For the thermoelectric kinetic coefficient,

$$\begin{aligned} P(Y) &= \int \frac{dv}{2\pi} e^{ivY} \chi(0, v) \\ &= \frac{1}{2\pi \sqrt{\mathcal{J}_1 \mathcal{J}_3 - \mathcal{J}_2^2}} \exp\left(\frac{\mathcal{J}_2}{\mathcal{J}_1 \mathcal{J}_3 - \mathcal{J}_2^2} \frac{Y}{2}\right) \\ &\quad \times K_0\left(\frac{\sqrt{\mathcal{J}_1 \mathcal{J}_3}}{\mathcal{J}_1 \mathcal{J}_3 - \mathcal{J}_2^2} \frac{Y}{2}\right), \quad (A4) \end{aligned}$$

where K_0 is the modified Bessel function. Here it was important that $\lambda = \mathcal{J}_1 \mathcal{J}_3 / \mathcal{J}_2^2 = 1 + 1/(12x^2) \geq 1$, so the following relation could be used:

$$\int_{-\infty}^{\infty} \frac{dq}{2\pi} \frac{e^{iqz}}{\sqrt{(1+iq)^2 - \lambda(iq)^2}} = \frac{1}{\pi\sqrt{\lambda-1}} \exp\left(\frac{z}{\lambda-1}\right) K_0\left(|z| \frac{\sqrt{\lambda}}{\lambda-1}\right). \quad (\text{A5})$$

In combination with Eqs. (39a)–(39c) and with the facts that $\mathcal{J}_1 \mathcal{J}_3 = (\Delta^2/E_C^4)(4/3)(1+12x^2)/(1-4x^2)^4$, and $\mathcal{J}_1 \mathcal{J}_3 - \mathcal{J}_2^2 = (\Delta^2/E_C^4)(4/3)/(1-4x^2)^4$, Eq. (A4) gives Eq. (8). The joint probability distribution is given by

$$\begin{aligned} P(X, Y) &= \int \frac{du}{2\pi} \frac{dv}{2\pi} e^{iuX+ivY} \chi(u, v) = \\ &= \frac{\Theta(X)}{\sqrt{2\pi\mathcal{J}_1 X}} \int \frac{dv}{2\pi} \times \\ &\quad \times e^{ivY - [(1+2iv\mathcal{J}_2)^2 + 4v^2\mathcal{J}_1\mathcal{J}_3]X/(2\mathcal{J}_1)} \\ &= \frac{\Theta(X)}{4\pi X \sqrt{\mathcal{J}_1\mathcal{J}_3 - \mathcal{J}_2^2}} \times \\ &\quad \times \exp\left[-\frac{X}{2\mathcal{J}_1} - \frac{(2\mathcal{J}_2 X - \mathcal{J}_1 Y)^2}{8(\mathcal{J}_1\mathcal{J}_3 - \mathcal{J}_2^2)\mathcal{J}_1 X}\right]. \end{aligned} \quad (\text{A6})$$

From this, the distribution function for the thermopower can be obtained by introducing the variable $Z = Y/X$,

$$\begin{aligned} P(Z) &= \int \delta(Z - Y/X) P(X, Y) dX dY \\ &= \frac{(2\mathcal{J}_1/\pi)\sqrt{\mathcal{J}_1\mathcal{J}_3 - \mathcal{J}_2^2}}{4(\mathcal{J}_1\mathcal{J}_3 - \mathcal{J}_2^2) + (2\mathcal{J}_2 - \mathcal{J}_1 Z)^2}, \end{aligned} \quad (\text{A7})$$

which gives Eq. (7).

Finally, to describe the correlations of the random processes τ_x, ε_x at different x , it is sufficient to use representation (37), and calculate the characteristic functional

$$\begin{aligned} \mathcal{X}[u(x), v(x)] &= \left\langle \exp\left\{i \int [u(x)\tau_x + v(x)\varepsilon_x] dx\right\}\right\rangle = \\ &= \exp\left\{-\frac{1}{2} \int dx_1 dx_2 \mathcal{K}(x_1, x_2)\right\}, \end{aligned} \quad (\text{A8a})$$

$$\begin{aligned} \mathcal{K}(x_1, x_2) &= u(x_1)u(x_2) \frac{E_C}{\Delta} \sum_k F_{x_1}(\epsilon_k) F_{x_2}(\epsilon_k) + \\ &\quad + 2u(x_1)v(x_2) \frac{E_C^2}{\Delta} \sum_k F_{x_1}(\epsilon_k) \tilde{F}_{x_2}(\epsilon_k) + \\ &\quad + v(x_1)v(x_2) \frac{E_C^3}{\Delta} \sum_k \tilde{F}_{x_1}(\epsilon_k) \tilde{F}_{x_2}(\epsilon_k), \end{aligned} \quad (\text{A8b})$$

where the subscripts at $F(\epsilon_k), \tilde{F}(\epsilon_k)$ indicate that the values E_+, E_- , entering in Eqs. (36d), Eqs. (36e), should be taken at the corresponding value of x , see Eq. (18). Eqs. (A8a), (A8b) represent the characteristic functional of a pair of Gaussian random processes, whose pair correlators are given by Eqs. (12a)–(12c), obtained by evaluation of the sums in Eq. (A8b) using the rule (38).

-
- ¹ H. van Houten, L.W. Molenkamp, C. W. J. Beenakker, and C. T. Foxon, *Semicond. Sci. Tech.* **7**, B215 (1992).
 - ² C. L. Kane and M. P. A. Fisher, *Phys. Rev. Lett.* **76**, 3192 (1996).
 - ³ R. Fazio, F. W. J. Hekking, and D. E. Khmel'nitskii, *Phys. Rev. Lett.* **80**, 5611 (1998).
 - ⁴ G. Catelani and I. L. Aleiner, *Sov. Phys. JETP* **100**, 331 (2005).
 - ⁵ F. Giazotto, T. T. Heikkilä, A. Luukanen, A. M. Savin, and J. P. Pekola, *Rev. Mod. Phys.* **78**, 217 (2006).
 - ⁶ J. T. Muhonen, M. Meschke, and J. P. Pekola, *Rep. Prog. Phys.* **75**, 046501 (2012).
 - ⁷ H. Courtois, F. W. J. Hekking, H. Q. Nguyen, C. B. Winkelmann, *J. Low Temp. Phys.* **175**, 799 (2014).
 - ⁸ A. S. Vasenko, E. V. Bezuglyi, H. Courtois, and F. W. J. Hekking, *Phys. Rev. B* **81**, 094513 (2010).
 - ⁹ A. Ozaeta, A. S. Vasenko, F. W. J. Hekking, and F. S. Bergeret, *Phys. Rev. B* **85**, 174518 (2012).
 - ¹⁰ F. J. DiSalvo, *Science* **285**, 703 (1999).
 - ¹¹ A. Shakouri, *Annu. Rev. Mater. Res.* **41**, 399 (2011).

- ¹² R. S. Whitney, *Phys. Rev. Lett.* **112**, 130601 (2014).
- ¹³ B. Sothmann, R. Sánchez, and A. N. Jordan, *Nanotechnology* **26**, 032001 (2015).
- ¹⁴ I. L. Aleiner, P. W. Brouwer and L. I. Glazman, *Phys. Rep.* **358**, 309 (2002).
- ¹⁵ I. O. Kulik and R. I. Shekhter, *Sov. Phys. JETP* **41** 308 (1975).
- ¹⁶ C. W. J. Beenakker, *Phys. Rev. B* **44**, 1646 (1991).
- ¹⁷ D. V. Averin and A. A. Odintsov, *Sov. Phys. JETP* **69**, 766 (1989).
- ¹⁸ L. I. Glazman, K. A. Matveev, *JETP Letters* **51**, 484 (1990).
- ¹⁹ D. V. Averin and Yu. V. Nazarov, *Phys. Rev. Lett.* **65**, 2446 (1990).
- ²⁰ D. V. Averin and Yu. V. Nazarov, in *Single Charge Tunneling: Coulomb Blockade Phenomena in Nanostructures*, ed. by H. Grabert and M. H. Devoret, NATO ASI Series B 294 (Plenum, New York, 1992), pp. 217-247.
- ²¹ Provided that N is even. In the case of odd N , the change in the internal state of the island may reduce to flipping

- the spin of the unpaired electron; this leads to the Kondo effect which enhances the conductance in the odd- N valleys [L. I. Glazman and M. E. Raikh, JETP Lett. **47**, 452 (1988); T. K. Ng and P. A. Lee, Phys. Rev. Lett. **61**, 1768 (1988)].
- ²² I. L. Aleiner and L. I. Glazman, Phys. Rev. Lett. **77**, 2057 (1996).
- ²³ E. V. Sukhorukov, G. Burkard, and D. Loss, Phys. Rev. B **63**, 125315 (2001).
- ²⁴ C. W. J. Beenakker and A. A. M. Staring, Phys. Rev. B **46**, 9667 (1992).
- ²⁵ A. A. M. Staring, L. W. Molenkamp, B. W. Alphenhaar, H. van Houten, O. J. A. Buyk, M. A. A. Mabesoone, C. W. J. Beenakker, and C. G. Foxon, Europhys. Lett. **22**, 57 (1993).
- ²⁶ S. Möller, H. Buhmann, S. F. Godijn, and L. W. Molenkamp, Phys. Rev. Lett. **81**, 5197 (1998).
- ²⁷ A. S. Dzurak, C. G. Smith, M. Pepper, D. A. Ritchie, J. E. F. Frost, G. A. C. Jones, and D. G. Hasko, Solid State Comm. **87**, 1145 (1993).
- ²⁸ A. S. Dzurak, C. G. Smith, C. H. W. Barnes, M. Pepper, L. Martín-Moreno, C. T. Liang, D. A. Ritchie, and G. A. C. Jones, Phys. Rev. B **55**, R10197 (1997).
- ²⁹ M. Turek and K. A. Matveev, Phys. Rev. B **65**, 115332 (2002).
- ³⁰ R. Scheibner, E. G. Novik, T. Borzenko, M. König, D. Reuter, A. D. Wieck, H. Buhmann, and L. W. Molenkamp, Phys. Rev. B **75**, 041301(R) (2007).
- ³¹ B. Kubala, J. König, and J. Pekola, Phys. Rev. Lett. **100**, 066801 (2008).
- ³² J. Koch, F. von Oppen, Y. Oreg, and E. Sela, Phys. Rev. B **70**, 195107 (2004).
- ³³ G. Billings, A. D. Stone, and Y. Alhassid, Phys. Rev. B **81**, 205303 (2010).
- ³⁴ M. Jonson and G. D. Mahan, Phys. Rev. **181** 1336 (1980).
- ³⁵ C. E. Porter and R. G. Thomas, Phys. Rev. **104**, 483 (1956).
- ³⁶ Yu. V. Nazarov and Ya. M. Blanter, *Quantum transport*, (Cambridge University Press, 2009).
- ³⁷ M. L. Mehta, *Random matrices* (Elsevier, Amsterdam, 2004).